

Analytical theory of Doppler reflectometry in slab plasma model

E Z Gusakov and A V Surkov

Ioffe Institute, Politekhnicheskaya 26, 194021 St. Petersburg, Russia

E-mail: a.surkov@mail.ioffe.ru

Abstract. Doppler reflectometry is considered in slab plasma model in the frameworks of analytical theory. The diagnostics locality is analyzed for both regimes: linear and nonlinear in turbulence amplitude. The toroidal antenna focusing of probing beam to the cut-off is proposed and discussed as a method to increase diagnostics spatial resolution. It is shown that even in the case of nonlinear regime of multiple scattering, the diagnostics can be used for an estimation (with certain accuracy) of plasma poloidal rotation profile.

PACS numbers: 52.70.Gw, 52.35.Hr, 52.35.Ra

1. Introduction

One of widespread methods used nowadays for plasma rotation velocity measurements is Doppler reflectometry [1, 2, 3]. This technique provides measuring fluctuations propagation poloidal velocity which is often shown to be dominated by plasma poloidal rotation velocity [3]. The method is based on plasma probing with a microwave beam which is tilted in respect to plasma density gradient (see figure 1). A back-scattered signal with frequency differing from the probing one is registered by a nearby standing or the same antenna. The information on plasma poloidal rotation is obtained in this technique from the frequency shift of the backscattering (BS) spectrum which is supposed to originate from the Doppler effect due to the fluctuation rotation.

Analytical theory of Doppler reflectometry was developed in recent papers [4, 5, 6], using analytical approach in slab plasma model, which is reliable for elongated plasma of large tokamaks. The linear case of probing wave single-scattering is considered there as well as the nonlinear process of the signal formation due to multi-scattering effect, which is essential for long probing ray trajectory, typical for large fusion devices. The diagnostics spatial and wavenumber resolution is determined and means to increase the method locality are discussed.

The present paper is devoted mainly to two following topics. First of all, we modify the linear theory of Doppler reflectometry taking into account possible antenna focusing in toroidal direction, which allows the diagnostics spatial resolution to be enhanced

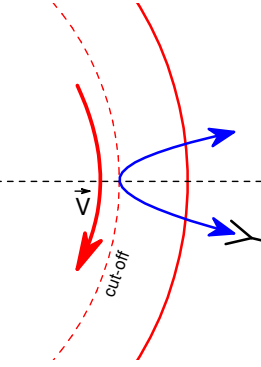


Figure 1. Diagnostics scheme.

without deteriorating the poloidal wavenumber selectivity, which takes place in case of poloidal focusing, discussed in [4]. Secondly, we compare the diagnostics locality in linear and non-linear regime and dwell upon experimental evidences, allowing us to distinguish these two cases.

2. Toroidal focusing in linear theory of Doppler reflectometry

In our consideration we follow our paper [4], taking into account possible antenna focusing in toroidal direction, which was not considered there. The study is made in the frameworks of geometrical optics (or WKB) approach, and the reader is referred to [4] for more accurate procedure, applied to the cut-off vicinity, where WKB approximation is not valid.

We consider normalized antenna electric field in the following form

$$\vec{E}_a(\vec{r}) = \vec{e}_z \int_{-\infty}^{+\infty} \frac{dk_y dk_z}{(2\pi)^2} W(x, k_y, k_z) f(k_y, k_z) e^{ik_y y + ik_z z}$$

where y, z axes denote poloidal and toroidal directions. Factor $f(k_y, k_z)$ takes into account the antenna pattern describing antenna radiation in vacuum

$$f(k_y, k_z) = \sqrt{\frac{c}{8\pi}} \int_{-\infty}^{+\infty} dy dz E_0(x=0, y, z) e^{-ik_y y - ik_z z}$$

where E_0 is vacuum antenna field, differing from E_a by the absence of the reflected wave contribution. We consider tilted gaussian antenna pattern

$$f(k_y, k_z) = 2\sqrt{\pi\rho_y\rho_z} \exp \left\{ -\frac{1}{2} \left[\rho_y^2 (k_y - \mathcal{K})^2 + \left(\rho_z^2 - \frac{ic\mathcal{R}}{\omega} \right) k_z^2 \right] \right\} \quad (1)$$

where a possibility to provide antenna focusing in toroidal direction is taken into account. Corresponding parameter \mathcal{R} in case of

$$\frac{c\mathcal{R}}{\omega} \gg \rho_z^2 \quad (2)$$

has a meaning of a wavefront curvature radius at the antenna. In (1) \mathcal{K} corresponds to the antenna tilt ($\mathcal{K} = \omega/c \sin \vartheta$, where ϑ denotes tilt angle in respect of the density gradient).

According to [7] radial distribution of ordinary wave electric field in WKB-approximation has the following form:

$$W(x, k_y, k_z) = 4 \sqrt{\frac{2\pi\omega}{c^2 k_x(x, k_y, k_z)}} \exp \left[i \int_0^{x_c(k_y, k_z)} k_x(x', k_y, k_z) dx' - \frac{i\pi}{4} \right] \\ \times \cos \left[\frac{\pi}{4} - \int_x^{x_c(k_y, k_z)} k_x(x', k_y, k_z) dx' \right]$$

where $k_x^2(x, k_y, k_z) = k^2(x) - k_y^2 - k_z^2 = [\omega^2 - \omega_{pe}^2(x)]/c^2 - k_y^2 - k_z^2$, the turning point $x_c(k_y, k_z)$ is determined by the equation

$$k_x[x_c(k_y, k_z), k_y, k_z] = 0$$

and $x = 0$ corresponds to the plasma border.

The scattering signal according to reciprocity theorem [8, 9] can be written as

$$A_s(\omega_s) = \frac{ie^2}{4m_e\omega} \sqrt{P_i} \int_{-\infty}^{+\infty} \delta n_\Omega(\vec{r}) E_a^2(\vec{r}) d\vec{r}$$

where P_i is the probing wave power and $\delta n_\Omega(\vec{r})$ is the density fluctuation with frequency Ω .

Using the same procedure as described in [4] we consider the turbulence to be slightly inhomogeneous along x direction and rotating with plasma in the poloidal direction, so that the density fluctuation correlation function takes the form

$$\langle \delta n(x, y, t_1) \delta n(x', y', t_2) \rangle = \delta n^2 \left(\frac{x+x'}{2} \right) \int_{-\infty}^{+\infty} \frac{d\boldsymbol{\varkappa} dq d\Omega}{(2\pi)^3} |\tilde{n}(\boldsymbol{\varkappa}, q, \Omega)|^2 \\ \times \exp \left[i\boldsymbol{\varkappa}(x-x') + iq(y-y') - i\Omega(t_1-t_2) - iqv \left(\frac{x+x'}{2} \right) (t_1-t_2) \right] \quad (3)$$

where $v(x)$ is the radial distribution of the plasma poloidal velocity. This allows us to obtain a spectral power density of the received signal in the following form [4]

$$p(\omega_s) = \langle |A_s|^2 \rangle = P_i \int_{-\infty}^{+\infty} dx \delta n^2(x) S(x) \quad (4)$$

The scattering efficiency $S(x)$ can be shown to consist of backscattering (BS) and forward scattering (FS) contributions

$$S(x) = \frac{1}{2} \left(\frac{e^2}{m_e c^2} \right)^2 \int_{-\infty}^{+\infty} \frac{dq}{2\pi} [S_{BS}(x, q) + S_{FS}(x, q)]$$

where

$$S_{BS}(x, q) = \frac{|f(-q/2, 0)|^4}{k_x^2(x, \mathcal{K}, 0)} \sum_{m=\pm 1} |\tilde{n}[2mk_x(x, \mathcal{K}, 0), q, \Omega - qv(x)]|^2 \\ \times \left\{ \rho_y^4 + \frac{c^2}{\omega^2} [\Lambda_0 + m\Lambda(x)]^2 \right\}^{-1/2} \left\{ \rho_z^4 + \frac{c^2}{\omega^2} [\Lambda_0 - \mathcal{R} + m\Lambda(x)]^2 \right\}^{-1/2} \quad (5)$$

Here $m = \pm 1$ corresponds to BS after and before the cut-off in respect of the probing ray propagation. The FS efficiency takes the form

$$S_{FS}(x, q) = 2 \left\{ \rho_y^4 + \frac{c^2}{\omega^2} \Lambda_0^2 \right\}^{-1/2} \left\{ \rho_z^4 + \frac{c^2}{\omega^2} (\Lambda_0 - \mathcal{R})^2 \right\}^{-1/2} \left| f \left(-\frac{q}{2}, 0 \right) \right|^4 \times \exp \left\{ -\frac{1}{2} \left[\frac{\rho_y q \Lambda(x)}{\Lambda_0} \right]^2 \right\} k_x^{-2}(x, \mathcal{K}, 0) \left| \tilde{n} \left[\frac{q^2 \Lambda(x)}{2k(x)\Lambda_0}, q, \Omega - qv(x) \right] \right|^2 \quad (6)$$

where

$$\Lambda(x) = \frac{\omega}{c} \int_x^{x_c(\mathcal{K}, 0)} \frac{dx'}{k_x(x', \mathcal{K}, 0)}, \quad \Lambda_0 \equiv \Lambda(0)$$

We consider expressions (5), (6) from the diagnostics locality point of view. First of all, the locality is determined by reversed square of the radial wavenumber $k_x^{-2}(x, \mathcal{K}, 0)$. This factor, corresponding to WKB-behavior of antenna electric field, underlines the cut-off vicinity, but for unfavorable density profiles, for example, linear or bent down ones, it does not suppress enough plasma periphery contribution. For the BS the second factor is fluctuations spectral density $|\tilde{n}[\pm 2k_x(x, \mathcal{K}, 0), q, \Omega]|^2$. Due to the dominance of long scales in the turbulence spectrum this factor underlines the cut-off vicinity, where $k_x(x, \mathcal{K}, 0)$ is small. For FS contribution the signal suppression due to the acquisition by antenna pattern periphery, described by the factor

$$\exp \left\{ -\frac{1}{2} \left[\frac{\rho_y q \Lambda(x)}{\Lambda_0} \right]^2 \right\}$$

plays an analogical role, it underlines the cut-off vicinity, where $\Lambda(x)$ is small.

Additional localization for BS contribution can be provided by antenna focusing to the cut-off, which occurs at $\mathcal{R} = \Lambda_0$. If the beam is narrow enough in toroidal direction, so that condition (2) is satisfied for $\mathcal{R} = \Lambda_0$, the factor

$$\left\{ \rho_z^4 + \frac{c^2}{\omega^2} [\Lambda_0 - \mathcal{R} + m\Lambda(x)]^2 \right\}^{-1/2} = \left\{ \rho_z^4 + \left[\frac{c\Lambda(x)}{\omega} \right]^2 \right\}^{-1/2}$$

is large in the cut-off vicinity. It should be noted that, the focusing in the poloidal direction can not give us such an effect, due to the fact, that we can not provide narrow antenna beam in poloidal direction without deteriorating the diagnostics poloidal wavenumber selectivity, which is described by $|f(-q/2, 0)|^4$.

Considering toroidal focusing influence on the FS efficiency, it should be noted that the focusing increases the amplitude of FS signal (6), but does not improve its locality.

The influence of the factors discussed on the spectrum of the registered signal is illustrated in the modelling, described in [4], and the results can be found below in section 4 (see figure 3 and figure 4) in comparison with spectra, modelled in nonlinear diagnostics regime. Now let us dwell upon the spectrum modelling, illustrating the antenna toroidal focusing influence. We consider the density profile of DIII-D tokamak plasma with internal transport barrier (figure 2(a)) [10]. The probing is performed at different frequencies and therefore with different cut-off positions. Here we take

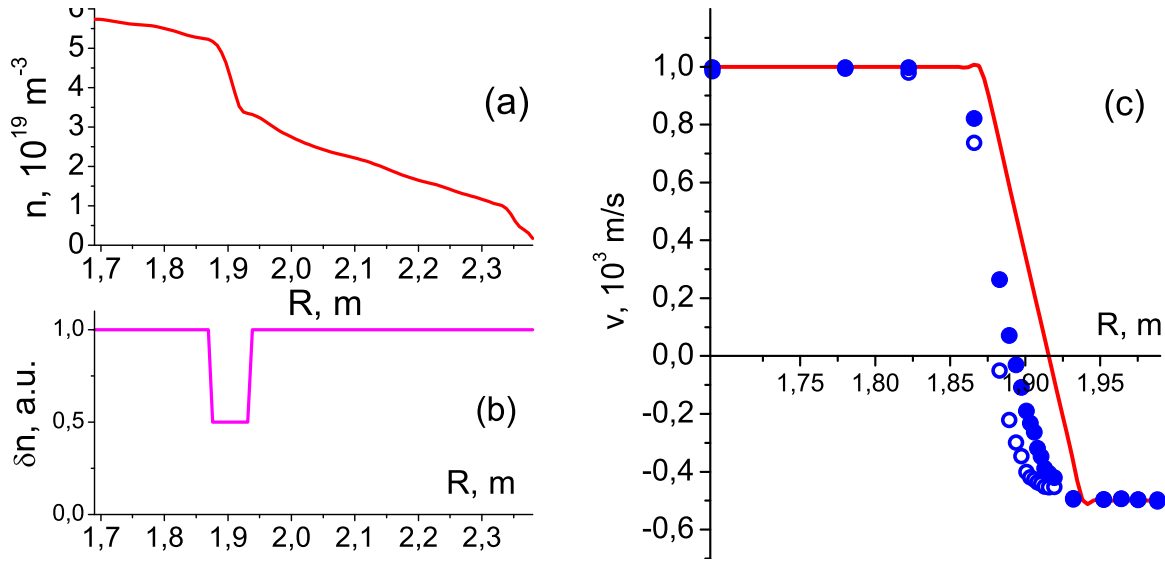


Figure 2. Antenna focusing influence. (a) DIII-D density profile [10]. (b) Turbulence amplitude assumed. (c) Poloidal velocity profile (—), and velocity estimated using Doppler reflectometry signal frequency spectrum shift: •—using antenna focusing, ○—without focusing.

into account the distance between antenna and the plasma, which was assumed to be equal 1 m, and suppose that focusing is performed into narrow in the toroidal direction spot ($\rho_z \sim 1$ cm) to provide condition (2) to be satisfied for $\mathcal{R} = \Lambda_0$. Besides that we take into account the turbulence suppression in the barrier region (see figure 2(b)).

Despite the fact that density profile in the barrier region is favorable for the diagnostics [4], antenna focusing makes the spectrum shift more adequate to the behavior of plasma velocity in the cut-off.

3. Nonlinear theory of Doppler reflectometry

In the section we review briefly the nonlinear analytical theory of Doppler reflectometry, which is considered in details in [5, 6]. In case of long enough trajectory length and sufficient turbulence amplitude, when the following criterion [11]

$$\gamma \equiv \frac{\omega_i^2}{c^2} \left(\frac{\delta n}{n_c} \right)^2 x_c \ell_{cx} \ln \frac{x_c}{\ell_{cx}} \gtrsim 1 \quad (7)$$

is satisfied, where ω_i is the probing frequency, $\delta n/n_c$ is the turbulence amplitude, normalized to the density in the cut-off, x_c is the distance to the cut-off, and ℓ_{cx} is the turbulence radial correlation length, we can neglect the BS during the wave propagation and consider multiple FS of the probing wave only. The density fluctuations in this case can be taken into account as a phase modulation during the probing wave propagation to the cut-off and backward. It can be shown that condition (7) holds true in large plasma devices even at small density perturbation level $\delta n/n_c \lesssim 10^{-2}$.

The wave electric field is determined by Helmholtz equation

$$\Delta E + [k^2(x) + \delta k^2(x, y, t)]E = 0$$

where

$$\delta k^2(x, y, t) = -\frac{\omega_i^2}{c^2} \frac{\delta n(x, y, t)}{n_c}$$

is the fluctuation of the wavenumber (here it is given for ordinary wave, but it can be easily written for extraordinary wave too). The electric field can be represented in the following form

$$E(l, y) = \int_{-\infty}^{+\infty} G[l, y|0, y_0; t] E_a^{(i)}(y_0) dy_0 \quad (8)$$

where l is a coordinate along the ray trajectory and

$$G[l, y|0, y_0; t] = \sqrt{\frac{\omega_i}{2\pi cl}} \exp \left\{ \frac{i\omega_i}{2c} \left[\frac{(y - y_0)^2}{l} - \frac{1}{n_c} \int_0^l n[x(l'), y^{(0)}(l'), t] dl' \right] - \frac{i\pi}{4} \right\}$$

Equation (8) describes the transportation of initial condition from the plasma border, where probing antenna is situated, inside the plasma along the ray trajectory. A function G contains the turbulence phase shift in question, which is determined by the density fluctuations and represents multiple FS effect.

According to the reciprocity theorem [8, 9], the registered signal is determined as an integral over all plasma border of the wave reflected by the cut-off

$$A_s = \frac{c}{16\pi} \int_{-\infty}^{+\infty} dy E(2\Lambda_0, y) E_a^{(r)}(y) \quad (9)$$

with a weight function, determined by the electric field of the acquisition antenna $E_a^{(r)}(y)$, if we consider it as probing one. Actually, due to narrow in the wavenumber space antenna pattern, the main component in this signal is formed due to the multiple FS, which changes essentially a poloidal wavenumber of the probing wave, meanwhile the radial wavenumber changes the sign due to reflection off the cut-off.

To obtain the spectrum of the registered signal and at the same time to analyze the diagnostics locality, as above we consider inhomogeneous turbulence, poloidally rotating with a plasma (3). Averaging $|A_s|^2$ (9) we obtain the spectrum in question [5, 6]

$$S(\omega) \propto \exp \left\{ -\frac{1}{2} \frac{\left[\omega - \omega_i + 2\mathcal{K} \left(\rho^{-2} + \hat{\mathcal{L}} q^2 \right)^{-1} \hat{\mathcal{L}} q^2 v \right]^2}{\hat{\mathcal{L}} (\Omega^2 + q^2 v^2) - \left(\rho^{-2} + \hat{\mathcal{L}} q^2 \right)^{-1} \left(\hat{\mathcal{L}} q^2 v \right)^2} \right\} \quad (10)$$

Here an operator $\hat{\mathcal{L}}$ has the meaning of the integration over distance from the plasma border to the cut-off, with the averaging over the turbulence spectrum

$$\begin{aligned} \hat{\mathcal{L}} \xi &\simeq \frac{\omega_i^2}{c^2 n_c^2} \int_0^{x_c} dx \delta n^2(x) \int_{-\infty}^{+\infty} \frac{d\boldsymbol{\varkappa} dq d\Omega}{(2\pi)^3} |\tilde{n}(\boldsymbol{\varkappa}, q, \Omega)|^2 \xi \\ &\times \begin{cases} \omega_i^2 / c^2 \delta(\boldsymbol{\varkappa}) k^{-2}(x), & x_c - x > \ell_{cx}/4 \\ 4L, & x_c - x \leq \ell_{cx}/4 \end{cases} \end{aligned} \quad (11)$$

where $L = [d \ln n_e(x)/dx|_{x=x_c}]^{-1}$ is the density variation scale in the cut-off. The integration in (11) is performed with a weight function, proportional to the inhomogeneous turbulence amplitude, and the factor, underlying the cut-off vicinity.

To analyze this expression for signal spectrum we consider simple case of homogeneous plasma poloidal rotation $v(x) = v$, which gives $\hat{\mathcal{L}}q^2v = v\hat{\mathcal{L}}q^2$. In case of strong nonlinear regime, when antenna beam divergence is completely determined by the turbulence ($\rho^2\hat{\mathcal{L}}q^2 \gg 1$) it can be seen that spectrum frequency shift is determined by traditional (linear) Doppler effect

$$\omega_{max} = \omega_i - 2\mathcal{K}v \quad (12)$$

On the contrary, the spectrum broadening

$$\Delta\omega = \sqrt{\hat{\mathcal{L}}\Omega^2}$$

is strongly influenced in nonlinear case by the turbulence amplitude and differs from linear one

$$\Delta\omega_{lin} = \left[\int_{-\infty}^{+\infty} \frac{d\boldsymbol{\varkappa} dq d\Omega}{(2\pi)^2} |n(\boldsymbol{\varkappa}, q, \Omega)|^2 \Omega^2 \right]^{1/2}$$

by the factor, which can be estimated as $\Delta\omega/\Delta\omega_{lin} \sim \gamma$, where γ is determined by (7). Thus in nonlinear case the frequency spectrum width can be substantially larger than in linear situation, when the factor γ is similar or less than 1.

In case of inhomogeneous plasma poloidal rotation the spectrum frequency shift is actually determined by the specifically averaged rotation velocity

$$\omega_{max} = \omega_i - \frac{2\mathcal{K}\hat{\mathcal{L}}q^2v}{\rho^{-2} + \hat{\mathcal{L}}q^2} \quad (13)$$

In this case the frequency spectrum shift can be produced by the region with high amplitude of the turbulence as well as by the region with high poloidal velocity.

The frequency spectrum broadening, which in case of homogeneous plasma poloidal rotation is caused by intrinsic frequency spectrum of fluctuations, is influenced here by additional factor associated with poloidal rotation inhomogeneity.

$$\Delta\omega = \left[\hat{\mathcal{L}}(\Omega^2 + q^2v^2) - \frac{(\hat{\mathcal{L}}q^2v)^2}{\rho^{-2} + \hat{\mathcal{L}}q^2} \right]^{1/2}$$

4. Discussion

At first, we consider the spectrum modelling, which was carried on according to the results of linear and nonlinear consideration of the Doppler reflectometry.

In calculation the following assumptions are made:

- (i) Geometrical parameters taken correspond to Tore Supra experiments [1]: $\omega_i/c \sim 12 \text{ cm}^{-1}$, $\rho \sim 14 \text{ cm}$, $\vartheta \sim 11.5^\circ$ distance to the cut-off $L \sim 20 \text{ cm}$.

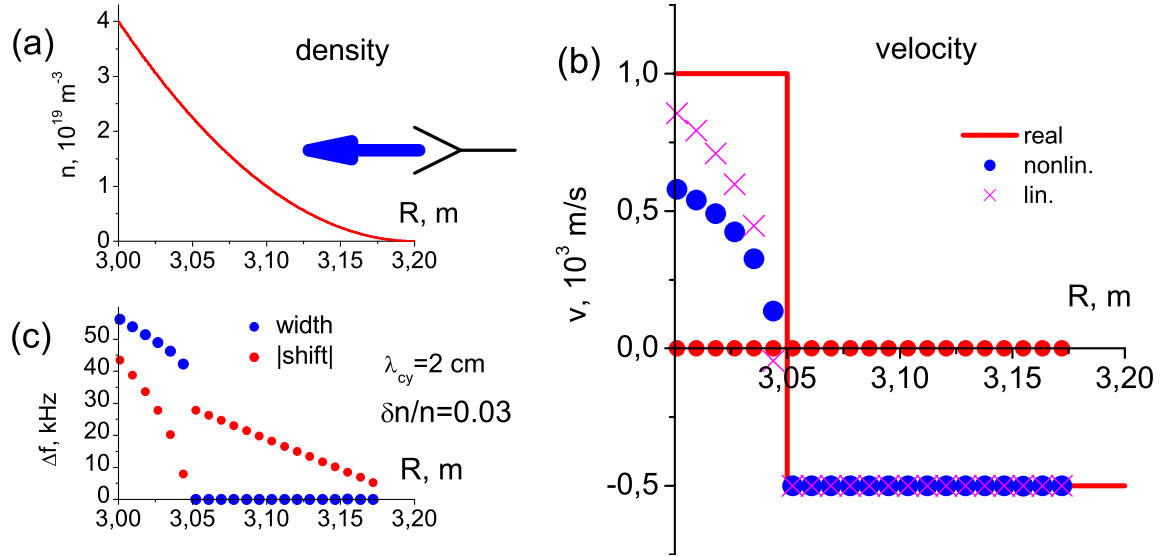


Figure 3. The signal spectrum evolution. (a) Assumed density profile. R denotes the major radius. (b) Assumed poloidal velocity profile (—), cut-off positions (●) and measured poloidal velocity profile in nonlinear (●) and linear (×) diagnostics regimes. (c) Absolute value of frequency shift (●) and width (●) of signal spectrum related to different probing frequencies (plotted via corresponding cut-off position).

- (ii) We consider the same antenna for the probing and reception. The probing is performed at different frequencies and therefore with different cut-off positions.
- (iii) For the sake of simplicity we suppose the turbulence level to be uniform ($\tilde{n} = 0.03$) and its wavenumber spectra to be gaussian. The fluctuations are believed to be low-frequency to neglect the spectrum width in case of homogeneous poloidal velocity profile.

First of all we consider plasma density profile (figure 3(a)) similar to observed in Tore Supra [12] and step-like plasma poloidal velocity distribution (figure 3(b)). The registered signal frequency shift (figure 3(c)) is calculated using (13), but, as it is usually done in experiment results interpretation, the measured poloidal velocity profile (figure 3(b)) is deduced from frequency spectrum shift using equation (12) for traditional (linear) Doppler effect in assumption that the registered signal spectrum shift corresponds to velocity in the cut-off.

It can be seen that the value of poloidal velocity measured in such a way coincides with assumed one in case of homogeneous poloidal velocity distribution and differs from it when the cut-off is situated in the region of variable velocity. In this case large contribution to the $\hat{\mathcal{L}}q^2v$ value is made by far from the cut-off regions due to unfavorable bent-down density profile, leading to the obscuration of the velocity in the cut-off. Thus such an interpretation of the diagnostics results gives the value of the poloidal velocity averaged in a specific way over plasma volume.

The frequency spectrum shift is compared in figure 3(c) with spectrum width, calculated for $\ell_{cy} \sim 2 \text{ cm}$. It can be seen that spectrum width can be larger than

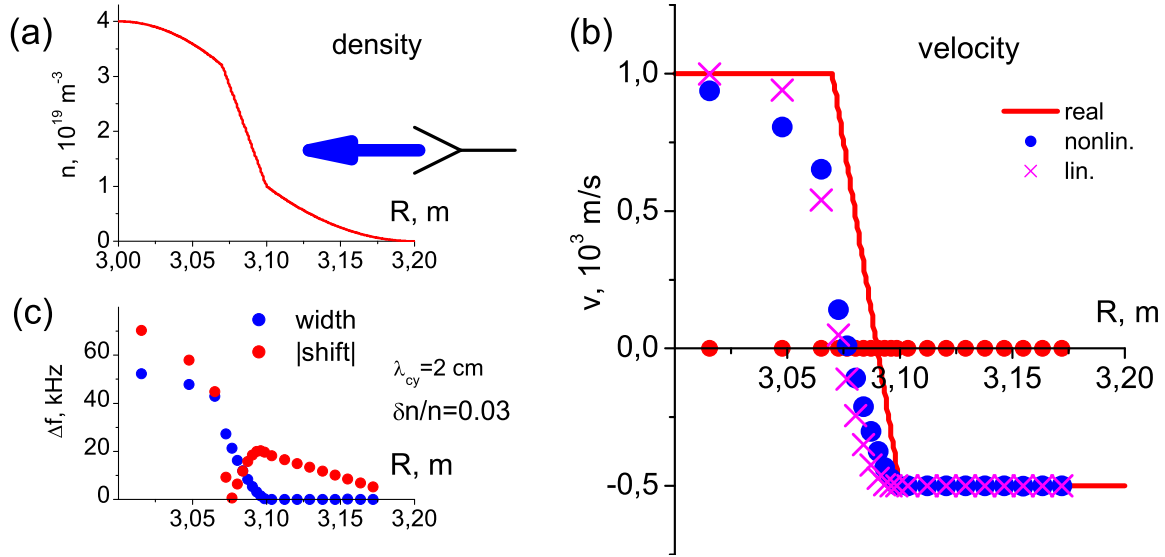


Figure 4. The signal spectrum evolution. (a) Assumed density profile. R denotes the major radius. (b) Assumed poloidal velocity profile (—), cut-off positions (●) and measured poloidal velocity profile in nonlinear (●) and linear (×) diagnostics regimes. (c) Absolute value of frequency shift (●) and width (●) of signal spectrum related to different probing frequencies (plotted via corresponding cut-off position).

frequency spectrum shift, which is typical for Doppler reflectometry experimental results. Besides, figure 3(c) demonstrates the spectrum width behavior which was described above: the spectrum is not broadened when probing wave propagates only in the region with homogeneous poloidal velocity (here we neglected the broadening, which arises due to intrinsic frequency spectrum of the turbulence) and broadens, when the cut-off, which is the bound of propagation region, crosses the point, where the velocity changes.

In addition, in figure 3(b) we compare the diagnostics results in linear and nonlinear regimes. In the both cases the plasma density profile is unfavorable for the diagnostics spatial resolution, but one can see that nonlinear regime is more problematic from the results interpretation point of view.

The second example is to emphasize the importance of plasma density profile for frequency spectrum formation. We consider plasma density profile (figure 4(a)) bent down in plasma periphery and bent up in the core. The poloidal velocity profile has high gradient in the ‘barrier’ region (figure 4(b)). It is easy to see that bent-up density profile underlines the cut-off contribution and improves the locality of the method. Also this effect is essential for linear Doppler reflectometry [4]. It leads to the fact that in case of favorable density profile the poloidal velocity profile measured by Doppler reflectometry corresponds to the certain extent to the real one.

Let us discuss the situation when the nonlinear theory developed should be applied. The nonlinear regime of Doppler reflectometry diagnostics is considered in the present paper, when multiple FS influence is essential for registered signal spectrum formation.

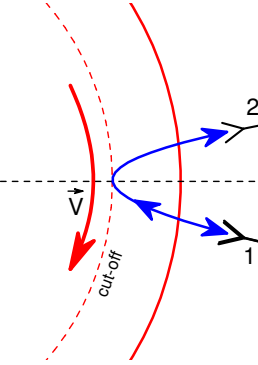


Figure 5. Diagnostics scheme. 1—emitting and receiving antenna, 2—additional receiving antenna.

For this situation to take place, two important criteria should be satisfied. At first, the turbulence amplitude is to be large enough to provide essential turbulent phase shift during the wave propagation, which is described by criterion (7).

The second condition leading to the necessity of nonlinear theory application to the diagnostics results is that small-angle scattering contribution is substantial in the received signal. This means that small-angle scattering signal amplitude should be comparable or larger than BS signal, formed by linear mechanism. Multiple small-angle scattering contribution (9) can be evaluated as

$$\langle |A_s|^2 \rangle \sim \frac{P_i \omega_i \ell_{cy}^2}{4 c x_c \gamma} \exp \left\{ -\frac{2\mathcal{K}^2 \ell_{cy}^2}{\gamma^2} \right\}$$

The BS signal amplitude (4) can be estimated as

$$\langle |A_s^{lin}|^2 \rangle \sim \frac{P_i}{2\sqrt{2\pi}} \gamma \frac{\omega_i \rho}{c x_c} |n(-2\mathcal{K})|^2$$

Here $|n(q)|^2$ is the fluctuation poloidal wavenumber spectrum. The ratio of the signal amplitudes

$$\alpha \equiv \frac{\langle |A_s|^2 \rangle}{\langle |A_s^{lin}|^2 \rangle} \sim \frac{\ell_{cy}^2}{\rho \gamma^2} \frac{\exp \left\{ -2\mathcal{K}^2 \ell_{cy}^2 / \gamma^2 \right\}}{|n(-2\mathcal{K})|^2}$$

For example, we consider turbulence spectral density $|n(q)|^2 = 4\pi \ell_{cy} [1 + q^2 \ell_{cy}^2]^{-3/2}$, where $\ell_{cy} \sim 2$ cm, probing frequency $f = \omega_i/2\pi = 60$ GHz, tilt angle $\theta = 30^\circ$, $\rho = 2$ cm. Then if $\gamma \sim 20$ the small-angle scattering contribution larger than BS one: $\alpha \sim 1.5$.

To conclude, we consider the experimental evidences of linear or nonlinear regime. A reliable criteria, which is actually very difficult to realize in experiment, is the spectrum of the passed, reflected off the cut-off signal. If the probing line can be distinguished in the spectrum of the signal, registered by antenna 2 in figure 5, we deal with linear regime of the scattering. In other case, when the probing line can not be observed in the broadened spectrum, the diagnostics works in nonlinear regime.

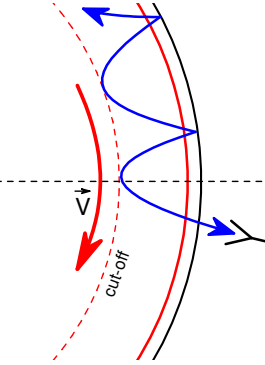


Figure 6. Multi-scattering in small toroidal device.

Another way to recognize the scattering regime is to compare BS signal spectrum width with one, provided by the antenna pattern due to the Doppler effect. In case of more broadened spectrum we deal with nonlinear regime of scattering.

The criteria of nonlinear theory applicability discussed can be usually satisfied in large toroidal devices. But we should note that the nonlinear regime can be realized in small tokamak due to possible reflection of the probing signal off the chamber wall (this effect for FT-2 tokamak was investigated experimentally in [13]). It leads to the effective increase of the ray trajectory, which can provide the satisfaction of the criterion (7). The signal spectrum of the signal can be estimated in this case using the results of our consideration (10), but the operator $\hat{\mathcal{L}}$ (11) should be multiplied by the quantity of the reflections off the plasma and wall.

5. Conclusion

In the present paper the Doppler reflectometry is considered in slab plasma model in the frameworks of analytical theory. The diagnostics locality is analyzed for linear and nonlinear regime. The toroidal beam focusing to the cut-off is proposed and discussed as a method to increase diagnostics spatial resolution.

In nonlinear diagnostics regime frequency spectrum shift and width of registered backscattered signal is analyzed in dependence on plasma density profile, turbulence spatial distribution and spectrum and plasma poloidal velocity profile. It is demonstrated that the frequency shift is not influenced by turbulence absolute amplitude and gives an information on poloidal velocity averaged over the vicinity of the cut-off, the size of which depends on the density profile and turbulence distribution.

Thus, even in the complicated situation of multi-scattering dominance Doppler reflectometry technique is proved to be able to give realistic information on plasma rotation. The spatial resolution of the diagnostics, however, suffers from transition to this nonlinear regime of scattering. The consideration presented allows the spatial resolution of the method to be analyzed for real experimental conditions, and thus the diagnostics results to be adequately interpreted.

Acknowledgments

The support of RFBR grants 02-02-17589, 04-02-16534, INTAS grant 01-2056 and NWO-RFBR grant 047.016.015 is acknowledged. A.V. Surkov is thankful to the “Dynasty” foundation for supporting his research.

References

- [1] Zou X L, Seak T F, Paume M, Chareau J M, Bottereau C and Leclert G 1999 *Proc. 26th EPS Conf. on Contr. Fusion and Plasma Physics (Maastricht)* ECA vol **23J** 1041
- [2] Bulanin V V, Lebedev S V, Levin L S and Roytershteyn V S 2000 *Plasma Phys. Rep.* **26** 813
- [3] Hirsch M, Holzhauer E, Baldzuhn J, Kurzan B and Scott B 2001 *Plasma Phys. Control. Fusion* **43** 1641
- [4] Gusakov E Z and Surkov A V 2004 *Plasma Phys. Control. Fusion* **46** 1143
- [5] Gusakov E Z, Surkov A V and Popov A Yu 2004 *Proc. 31st EPS Conference on Plasma Phys (London)* ECA vol **28B** P-1.182.
- [6] Gusakov E Z and Surkov A V 2004 *Submitted to Plasma Phys. Control. Fusion*
- [7] Gusakov E Z and Tyntarev M A 1997 *Fusion Eng. Design* **34** 501
- [8] Ginzburg V L 1970 *The Propagation of Electromagnetic Waves in Plasmas* (Oxford:Pergamon)
- [9] Piliya A D and Popov A Yu 2002 *Plasma Phys. Control. Fusion* **44** 467
- [10] Doyle E J, Staebler G M, Zeng L, Rhodes T L, Burrell K H, Greenfield C M, Groebner R J, McKee G R, Peebles W A, Rettig C L, Rice B W and Stallard B W 2000 *Plasma Phys. Control. Fusion* **42** A237
- [11] Gusakov E Z and Popov A Yu 2002 *Plasma Phys. Control. Fusion* **44** 2327
- [12] Clairet F, Bottereau C, Chareau J M, Paume M and Sabot R 2001 *Plasma Phys. Control. Fusion* **43** 429
- [13] Altukhov A B, Bulanin V V, Gurchenko A D, Gusakov E Z, Esipov L A, Selenin V L and Stepanov A Yu *Proc. 30th EPS Conference on Contr. Fusion and Plasma Phys., St. Petersburg, 7-11 July 2003 ECA Vol. 27A, P-2.57*